10-2011

Another dimension from LiDAR – Obtaining foliage density from full waveform data

Thomas Adams
Scion, Rotorua, New Zealand

Peter Beets
Metservice, 30 Salamanca Road, Kelburn, Wellington 6012, New Zealand

Christopher Parrish
University of New Hampshire, Durham

Another dimension from LiDAR – Obtaining foliage density from full waveform data

Thomas Adams[1], Peter Beets[2], Christopher Parrish[3]

[1]Scion, 49 Sala Street, Rotorua, New Zealand. thomas.adams@scionresearch.com
[2]Scion, 49 Sala Street, Rotorua, New Zealand. peter.beets@scionresearch.com
[3]NOAA/NGS, JHC-CCOM, 24 Colovos Road, Durham, NH, USA. chris.parrish@noaa.gov

Abstract

LiDAR tells the user *where* surfaces are, not *what* they are. In this study we investigate the potential for waveform LiDAR to provide more information on the nature of the returns over forestry. Waveform LiDAR was acquired for ten *Pinus radiata* plots in a New Zealand plantation, along with comprehensive leaf area sampling in 2m vertical bands. The decay rate of each waveform peak was shown to be a useful tool for estimating foliage density, and has potential for identifying regions containing ground and understorey.

Leaf Area Density (LAD) is an expression of foliage density per unit height, and a relationship between waveform decay rate and LAD was developed with an R^2 of 56%. Incorporating the proportion of discrete LiDAR that fell in that band (which itself has an R^2 of 50%) improves this model to explain 69% of the variation in LAD. This is a good result, especially given the costs and difficulties in measuring leaf area directly. As foliage density varies dramatically on a fine scale it was not possible to differentiate the nature of every single LiDAR return – but by averaging over a small area local variation in LAD could be easily mapped.

Ground returns could be distinguished as having short decays, and broad leafed understorey typically had values between those of the canopy and ground, although surface roughness and slope make it impossible to robustly identify single returns. This study produced a useful model for estimating LAD in *Pinus radiata* which could easily be extended to other coniferous species.

Keywords

Waveform LiDAR, foliage density, Leaf Area Density, waveform shape, deconvolution

1. Introduction

1.1 Foliage measurement

Foliage is the engine that drives tree growth. Foliage may be used as a good measure of tree growth and carbon sequestration, but also of tree form and fire risk. Knowledge of the 3D distribution of foliage can be used for many applications, such as carbon accounting (Stephens 2007), growth and yield forecasting (Naesset 1997), fire modelling (Morsdorf *et al*. 2004) and biodiversity estimation (Hofton *et al*. 2006).

Direct measurement of foliage location for individual trees is time consuming, costly and not overly representative at a stand scale (Bongers 2001). More spatially integrated measures of foliage distribution have emerged with simpler formulations which can be easily included in further analyses. The most common of these are canopy cover, Leaf Area Index (LAI) and Leaf Area Density (LAD). Canopy cover is the projected area of canopy – as viewed from above - per unit area of ground. The maximum canopy cover value of 1 indicates that the canopy completely obscures the ground, or is 'closed'. Leaf Area Index goes further, and is the one-sided area of leaf tissue per unit of ground surface area (Watson 1947). Leaf Area Density extends this once more, and is defined as the total leaf area per unit ground area per unit height. Essentially, LAD is the vertical distribution of leaf area that in summation will equal the LAI.

LAI and LAD can only be measured exactly through destructive sampling of single trees. LAI can be estimated through litter collection and known tree-allometry, ground-based hemispherical photography and LiDAR, although none of these methods offer high levels of accuracy or have been used to resolve LAI into LAD (Forster and Nairn 2010). Of these methods LiDAR appears to offer the greatest potential because it provides a three dimensional characterisation of canopy (Lefsky *et al*. 1999).

1.2 LiDAR

LiDAR – or Light Detection and Ranging - has long been used for mapping large, continuous surfaces such as ground and buildings. Often aerial imagery is acquired at the same time to assist in surface identification. Recently LiDAR has found a home in forestry, where returns from the canopy add valuable information on the vertical structure of the forest as well as the ground beneath. For a thorough explanation of the function and application of LiDAR in forestry the reader is directed to Hyyppä *et al*. (2004), Lim *et al*. (2003) or Adams *et al*. (2011).

LiDAR systems can be separated into two classes: discrete-return and full-waveform. Discrete-return systems use hardware-based subsystems (e.g., a constant fraction discriminator and time interval meter) to extract and record ranges and intensities in real time for a few individual returns per transmitted pulse (typically less than 5). Full-waveform systems on the other hand, digitize the backscattered laser echo sampled over a set period (typically around 1ns), providing a complete record of received signal amplitude over time. These digitized waveforms are stored for subsequent processing and analysis, thereby enabling additional information to be extracted. This information can include not only additional ranges, but also metrics related to surface roughness, slope and other characteristics. Figure 1 gives an example of a digitized waveform. Note how the discrete returns occur slightly before the waveform peaks; this is due to the fact that the discrete-return ranging is based on identifying a point on the leading edge at which the amplitude is a constant fraction of the peak (e.g. the 50% point). In both discrete-return and full waveform systems, georeferenced point clouds can be produced using the extracted ranges, sensor position and orientation data, scan angle data, sensor model, and associated calibration parameters.

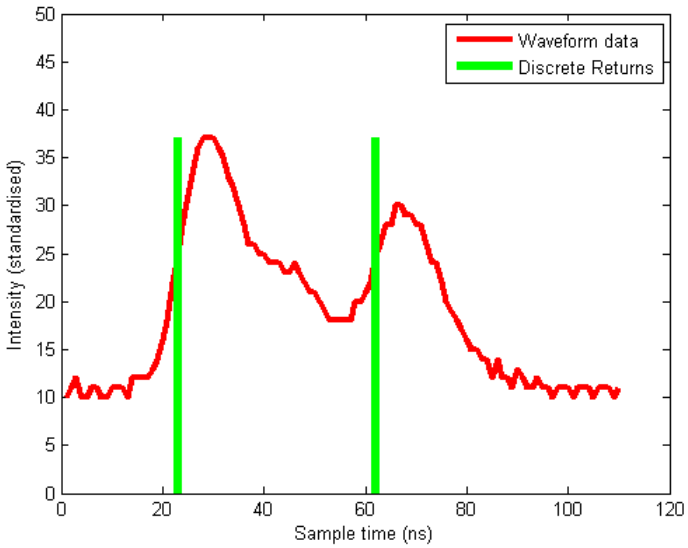

Figure 1 – An example of waveform and discrete-return LiDAR data

Canopy is not a flat impermeable surface like the ground, and it is this fact that allows us to collect information throughout its depth. Unlike in urban environments, where each return results from a single large surface, the scale of foliage is much less than that of the beam width (~0.2m) and vertical sampling interval (0.15m). Thus each return is due to the integrated reflections from a large cylinder of foliage. If the waveform digitizer has a nanosecond sampling period, then the

waveform at that point is due to the reflections from a biscuit tin sized volume of foliage of around $0.005m^3$. It should be noted that the return signal from each 'biscuit tin' depends not only on the foliage in that volume, but also on the attenuation of the beam by foliage above it. Multiple scattering events have been shown to be of negligible importance (Blair and Hofton 1999).

Some authors have attempted to investigate foliage density by considering the proportion of discrete returns per unit height. Morsdorf (2006) found a correlation between LAI measured by hemispherical photography and the proportion of discrete returns that hit the ground with an R^2 of 69%. This correlation was also found by Riaño (2004) on two sites in Spain. However, these studies give no information on the vertical distribution of the foliage, or LAD. Vertical canopy information from discrete LiDAR always suffers from the fact that the transmitted laser pulse width can be greater than 10ns, and there is typically a 'blind-spot' between returns of 1.2 - 3m during which no other returns can be counted (Reitberger, Krzystek, and Stilla 2008).

1.3 Full waveform LiDAR analysis

Full-waveform LiDAR can greatly reduce this blind spot by post-processing the waveform data to identify proximal peaks which would otherwise be treated as one (Parrish *et al*. 2011). Chauve *et al*. (2009) found 40-60% additional points in an Alpine coniferous forest. The most common approach is to approximate the waveform as a series of Gaussians, fitted by a non-linear least-squares approach (Hofton, Minster, and Blair 2000; Reitberger, Krzystek, and Stilla 2006), or expectation-maximisation (Persson *et al*. 2005). Wagner *et al*. (2006) found that fitting Gaussian peaks to the data could account for 98% of waveform shapes, although this was over an urban environment and he notes that Gaussians may not always be appropriate over vegetation.

Additional canopy points are not the only benefit of working with full-waveform data. The signal shape itself may yield information on the nature of the target. Whilst discrete LiDAR returns are given an intensity, the value is a function of transmitted power, range, atmospheric transmittance, system transmittance, receiver aperture, beam divergence, surface roughness, relative geometry between the sensor and target, and any attenuation due to foliage higher in the canopy. Studies have corrected for range and scan angle to derive a back-scattering cross section (Wagner *et al*. 2006), and for species identification between *Lodgepole Pine* and *Sitka Spruce* in Scotland (Donoghue *et al*. 2007). Reitberger used peak width and integral as clustering parameters to segment individual trees and group them according to species. The study achieved 80% accuracy in identifying deciduous and coniferous species (Reitberger, Krzystek, and Stilla 2006). Lin and Mills (2010) found pulse width less noisy than intensity for identifying surface roughness and slope. Like Wagner (2006), Chauve *et. al.* (2009) note that the waveform is often skewed, and that a Gaussian may not be appropriate in all cases. Experimentation with a lognormal distribution provided a better fit for some pulses over a forest, although a standard Gaussian was found to provide the best fit in 99.3% of cases. Generalised Gaussians were also used, which theoretically should provide a better fit than standard Gaussians, although this didn't occur due to the extra degrees of freedom and limitations of the optimisation algorithm.

Whilst other authors have noted this skewness of the waveform, in this study we use it to categorise returns. If we assume that the needles and branches within a sampled volume are sufficiently small and randomly orientated, then - as a simple model - the canopy can be imagined as a volume of semi-transparent gas. Whilst this is not a physical reality, it allows us to employ some modelling simplifications that allow a quantitative insight into the canopy's average properties. We can then assume that the canopy has – as a gas would – a reflectivity *R*, transmissivity *T*, and absorbance *A*. Thus transmission through the canopy can be modelled with the Beer-Lambert law

$$T = \frac{I_T}{I_0} = e^{-\alpha x} \tag{1}$$

Where I_T is the transmitted intensity, I_0 is the initial intensity, α is the absorption coefficient and x is the distance travelled through the gas. Note that whilst transmissivity and reflectivity are both

functions of wavelength, lasers are fundamentally limited to a single wavelength so we can ignore this and define our parameters at a wavelength of 1064nm. For an interesting investigation into multi-spectral LiDAR the reader is directed to Morsdorf *et al*. (2009).

At a depth x into the canopy, a constant proportion (R) of the incident light will be reflected. We assume Lambertian reflectance, and that this is further attenuated by the foliage-gas as it leaves. I_R at the surface is then given by

$$I_{R(surface)} = I_0 R e^{-2\alpha x} \tag{2}$$

Thus we see that if the canopy is of a constant density and distribution, we can expect an exponential decay in intensity characterised by a decay constant of 2α. For simplicity this decay constant will be called λ.

I_R as measured at the receiver is also a function of range as defined by the radar equation

$$I_{R(receiver)} = \frac{I_0 \sigma F^4}{(4\pi)^2(\rho+x)^4} \tag{3}$$

Where σ is the target scattering coefficient, F is the propagation factor which accounts for atmospheric loss, and ρ is the distance to the start of the foliage. So we may also see a fall off in I_R in the form of x^{-4}. However our study site was flown at a height of ρ~1000m, whereas x~2m, so $x<<\rho$ and it is reasonable to ignore this effect.

Jutzi and Stilla (2006) note that the return waveform *y(t)* is a convolution of the surface response *v(x,y,z)*, the transmitted waveform *o(t)*, the response of the measurement unit *m(t)* and the spatial beam distribution *p(x,y)*. If the pulse is timed and we know the plane position and scan angle in three dimensions (i.e. we can describe *x,y* and *z* as a function of *t*) then we can describe *v(x,y,z)* as *v(t)*. Furthermore, based on our simple isotropic gas model of the canopy locale, we can ignore *p(x,y)* but add in a background noise *n(t)* leaving

$$y(t) = v(t) * o(t) * m(t) + n(t) \tag{4}$$

Comparison of the outgoing waveform *o(t)* (sampled as standard with some waveform digitisers) with the return waveform *y(t)* for large flat surfaces (a pond on a windless day) shows that *m(t)* is negligible compared to *o(t)*. Thus we have

$$y(t) \approx v(t) * o(t) + n(t) \tag{5}$$

The surface response *v(t)* is what we are interested in determining, and equation (5) may be solved by a Wiener deconvolution where we estimate *g(t)* to minimise the error in our estimation of *v(t)* so that

$$\hat{v}(t) = g(t) * y(t) \tag{6}$$

The Weiner deconvolution filter can be used to find *g(t)*, shown here in the frequency domain

$$G(f) = \frac{O^*(f)S(f)}{|O(f)|^2 S(f) + N(f)} \tag{7}$$

Where *S(f)* is the mean power spectral density of the outgoing signal *o(t)*. *N(f)* is the power spectral density of the noise *n(t)*. This may be solved to obtain $\hat{v}(t)$, which will from hereon in be referred to as the deconvolved waveform.

The skewness of waveform profiles over foliage has been noted by several authors (Wagner *et al*. 2006; Chauve *et al*. 2009; Jutzi and Stilla 2006). In this study we define this skewness as an

exponential decay, which will be more apparent in the deconvolved waveform than the original as the blurring function of the outgoing pulse has been removed. In this study we test the hypothesis that the decay constant of the deconvolved waveform will correlate with the local foliage density, expressed as an LAD.

2. Method

2.1 Field data collection

The field data collection for this project was shared with that of Beets *et al*. (2011). Ten 0.16ha field plots of nine year-old *Pinus radiata* were selected for study. Each plot was planted with the same stocking in 1997, and had received the same silviculture. Five representative sample trees per plot were felled from 21st August - 8th September, 2006. Tree crowns were weighed fresh in the field by 2m height zone, measured from the base of each tree. Fifty needle fascicles were sampled randomly from each height zone and stored in polythene bags with water. Sample branches from each 2m height zone were weighed fresh in the field, and partially dried to aid with separation of needles from branches. Needles were oven dried to constant weight at 65 degrees C and weighed. Leaf area of the 50 fascicles per 2m height zone was determined on an all-surfaces basis from fascicle length and volume, using methods described in Beets and Lane (1987), and then oven-dried and weighed. LAD by 2m height zone was calculated for each zone by multiplying the fascicle dry weight by the specific leaf area of the 50 fascicles. The leaf area index per plot was obtained using the basal area ratio method, where the sum of zonal leaf areas of sample trees per plot is multiplied by the plot basal area divided by the sample tree basal area (Madgwick and Service 1981).

2.2 LiDAR data collection

The study site was flown by New Zealand Aerial Mapping on 9th June 2007, and measured with an Optech ALTM 3100EA LiDAR system and waveform digitiser with a sampling rate of 1ns. Raw GPS data and discrete LiDAR information was processed with REALM software into a Corrected Sensor Data (CSD) file. The waveform data was measured at 1ns intervals and provided as five swathes in Optech's NDF binary format with an IDX index file. Matlab code was adapted from Parrish (2007) to suit the updated NDF format and to georeference the waveforms according to New Zealand's NZGD2000 coordinate system.

2.3 Waveform analysis

Much work has been done on identifying and resolving peaks in waveform data (Chauve *et al*. 2009). In this work we are investigating the decay of the waveform, so separating closely-spaced peaks is of no use. For efficiency we use the discrete LiDAR dataset to identify peaks, and the waveform LiDAR to determine the decay rate. This process is detailed below.

Step 1

Read and georeference LiDAR data. Using adapted code from Parrish (2007) each sample in the waveform is assigned an *xyz* coordinate and compared with the field plot locations. Waveforms – or sections of waveforms – that fall within the field plot are written to a new file with their respective locations. In comparison with Parrish, the waveform is not deconvolved at this point, and all points within the sample areas are written to a text file. In addition the CSD file is read and the discrete LiDAR point cloud is extracted for the whole of Puruki forest.

Step 2

Subtract ground surface from LiDAR data. By subtracting the ground surface from the data we determine heights above ground instead of heights above sea-level, which is standard practice for determining information on canopy as opposed to terrain. In this paper we refer to this process as

'degrounding'. The discrete LiDAR data for the whole forest is used with FUSION's *GroundFilter.exe* function (McGaughey 2010) to determine a ground surface on a 1m grid. This gives a better result than using the clipped data for individual plots. This grid is then used to linearly interpolate a ground height for every waveform sample saved in the text file produced in step 1, and every discrete return that falls within the plot areas. For every plot a georeferenced degrounded waveform file is produced, along with a corresponding degrounded discrete point cloud.

Step 3

Deconvolve waveform. Each degrounded waveform file is read, and each waveform line individually analysed. A Wiener deconvolution (see introduction) is used, using the outgoing waveform as the deconvolution kernel. Note that the deconvolution increases the amount of noise, particularly away from peaks.

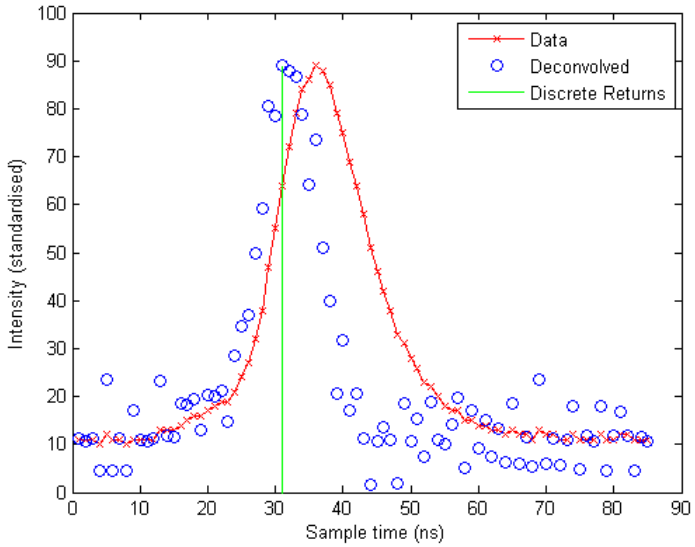

Figure 2. Original waveform and deconvolved waveform.

Step 4

Separate peaks and fit exponential decay. Peaks are identified as the nearest local maxima to each discrete return. As the discrete return is determined on the leading edge of a pulse, the local maxima should always be just after this point. In the instances where a waveform contains multiple peaks, the data between peaks is sampled from local maxima to local minima to find the exponential decay. The decay is found using a weighted least squares approach, where samples are weighted by their height (to encourage curve fitting to match the peaks as opposed to the background noise). Figure 3 shows a waveform with two returns and two fitted exponential decays. Note that the x axis is measured in time, not in height. If the decay were measured in height, waveforms travelling non-perpendicularly to the ground would appear compressed and hence have artificially increased decay constants (λ). Once the decay constants are found they are added to a point cloud output that includes xyz coordinates, intensity and λ.

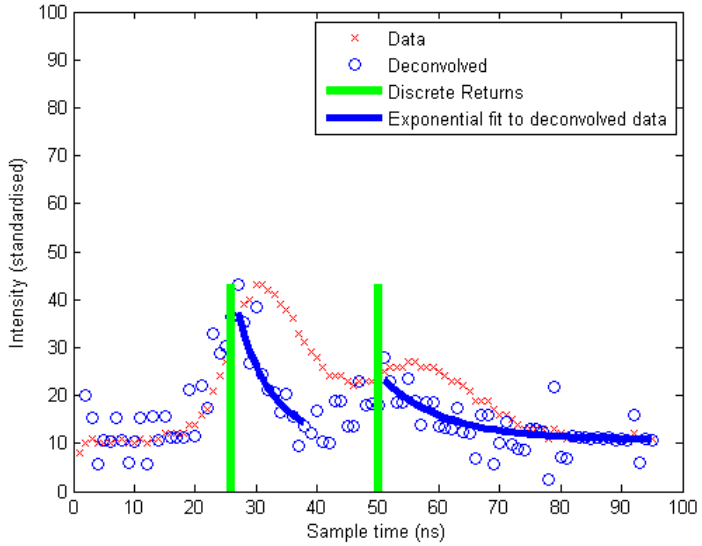

Figure 3. Example of multiple peak waveform with two exponential decays fitted.

3. Results

3.1 LAD vs. proportion of returns.

Extending the work of Morsdorf *et al*. (2006), we initially use the degrounded discrete LiDAR data to compare LAD with the proportion of LiDAR returns that occurred within each height band. Figure 4 shows the results provide a reasonable model (R^2 of 50%). This R^2 is not as good as the 69% found by Morsdorf *et. al.*, although their model considered net LAI as opposed the LAD at different height bands. Our model is also flawed in that it does not go through the origin – a LAD of 0 should lead to no returns.

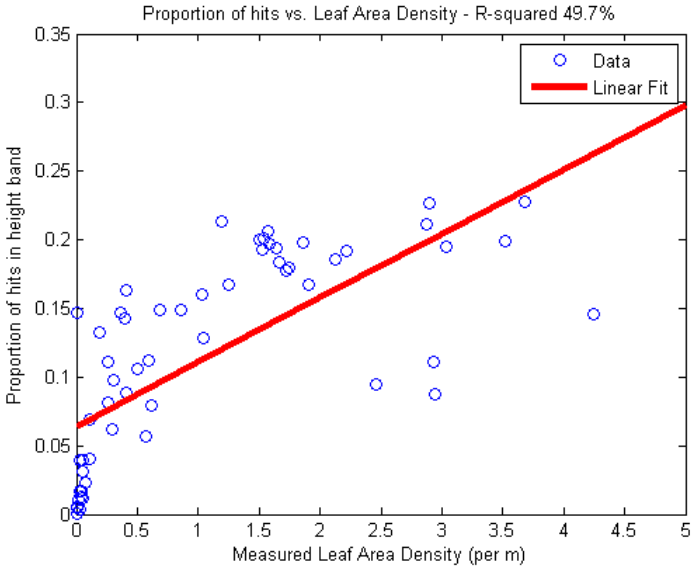

Figure 4 – Leaf Area Density vs. proportion of hits per height band

3.2 LAD vs. average decay rate

Within each height band there are many LiDAR returns. If our approximation of foliage being an isotropic gas were true, then we would expect all of the returns to exhibit the same decay. However this is only a simple model, and some pulses will hit dense areas of vegetation whereas others will find a gap and only receive a glancing blow. So each individual decay rate is not of

much use, but the average over the whole height band should be informative. Experiments with the mean and median showed that the mean is slightly more related to LAD, with an R^2 of 55.8% as opposed to 54.1% for the median. The correlation for the mean is illustrated in figure 5.

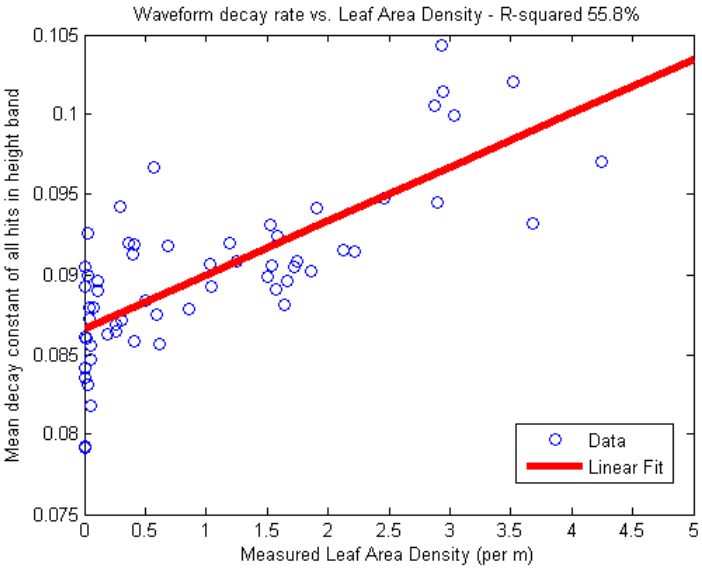

Figure 5 – Deconvolved waveform decay rate vs Leaf Area Density

This is a good result and shows that waveform decay rates are representative of LAD. It also yields the question whether this model could be improved by using the proportion of LiDAR returns as well as the mean decay constant. Assuming a simple linear model

$$L = \beta\bar{\lambda} + \gamma p + c \tag{8}$$

Where L is LAD, $\bar{\lambda}$ is mean decay constant, p is proportion of hits, c is a constant and β and γ are constants of proportionality. Solving this for a least-squares solution, we obtain the model shown in Figure 6, with a R^2 of 69%. This is a great improvement in accuracy, although it is apparent that the relationship is not perfectly linear, leading to underestimation at lower LAI values.

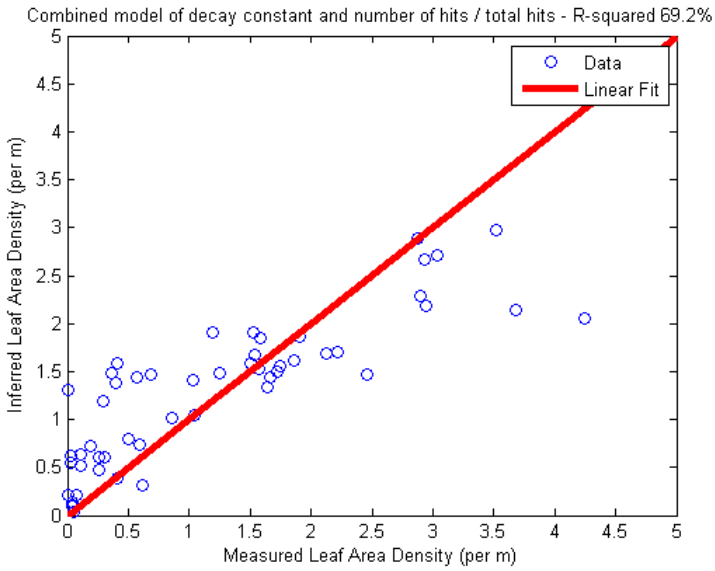

Figure 6 – Model for Leaf Area Density based on average decay constant and proportion of hits.

4. Discussion

The results show that modelling foliage as a semi-transparent gas and applying the Beer-Lambert law for transmittance enables reasonable estimates of the parameters of interest. A good correlation between Leaf Area Density and average decay rate $\bar{\lambda}$ was found, with an R^2 of 56%. Unfortunately, this simple model does not work for individual pulses. If it did, the decay rate could easily be used to differentiate returns from foliage to those from branches, the stem, understorey and the ground. Unfortunately - just like intensity - decay constant is still a function of slope, roughness and size. For each surface type there are so many variations and ways in which the light can hit it that only the mean of a large number of hits is useful. For example, light hitting a particularly dense patch of foliage would yield a shorter decay than light hitting hard ground at an oblique angle. The crucial difference between decay constant and intensity is that decay constant is not affected if the light beam has been attenuated prior to hitting the target. Figure 7 shows an attempt to correlate LAD with mean intensity within a height band, and the R^2 value of 2% shows that there is little or no correlation.

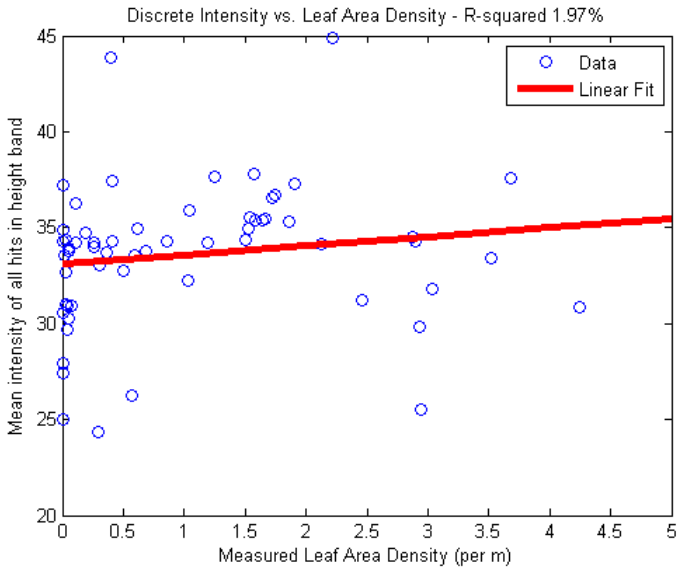

Figure 7 – Discrete return intensity vs. leaf area density.

When considering the average decay constant within a height band, there is a distinct change between foliage and ground. Figure 8 shows how LAD inferred from $\bar{\lambda}$ varies with height for plot 10, in 1m height bands, along with the measured LAD. Two trends are clear: The LiDAR method underestimates LAD at the very top of the tree, and grossly overestimates it at the base. The underestimation at the top of the tree is likely due to the fact that LiDAR does not sample everywhere, and the beam footprints are prone to missing the very tops of trees (Hyyppä *et al.* 2004). The overestimation at the base (where the measured LAD was 0) is due to the fact that understorey and ground returns also feature. Due to the broad-leafed nature of the understorey (ferns, grasses, and broad-leafed shrubs), these are likely to attenuate incident light faster than dispersed needles, and have a higher decay rate. The ground will attenuate light almost instantly, so can be expected to have an even higher decay rate. Understorey was recorded for plot 10 as approximately 70% cover up to a height of 4m. This result would be consistent with the increase in $\bar{\lambda}$ from this height onwards.

Unfortunately, as we have already mentioned, for each height band there exists a wide range of λ due to its dependence on surface roughness and slope. We cannot expect to separate out individual returns from understorey as distinct from canopy foliage, but an increase in $\bar{\lambda}$ can be used as an indicator of where understory begins. Higher values of $\bar{\lambda}$ could also be used to identify ground returns, but it is unlikely this method would be as effective as the well-researched surface fitting methods employed for digital terrain model extraction (see Hyyppä *et al.* (2004) for a history of

methods). Further research is necessary for applying this method in mixed species forests – it may for example be possible to gauge the species mix by the range in λ, particularly if it is a mix of coniferous and deciduous species.

This study has determined that – like intensity – waveform decay is a useful addition to a discrete LiDAR point set. Whilst each individual value does not determine the surface type for each individual return, when taken as a population over an area they can be useful – along with geometry and aerial photography – for identifying surface traits. A model for foliage density from LiDAR will be of use for carbon accounting, growth and yield, and fire risk modelling.

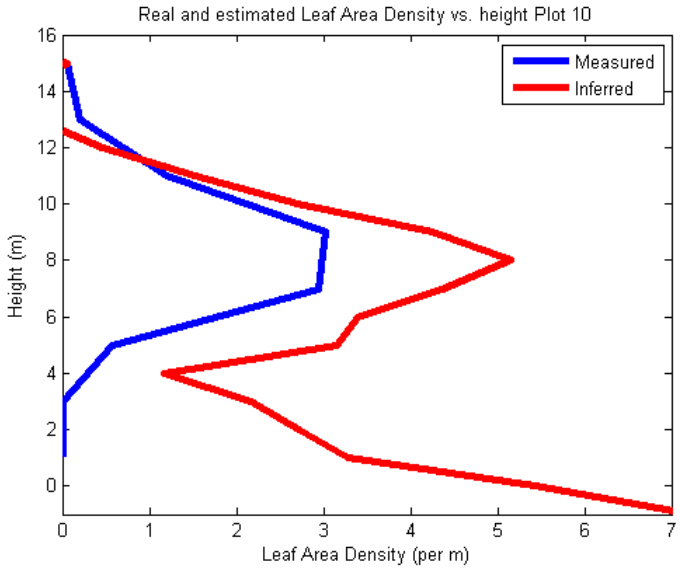

Figure 8 – Leaf Area Density (measured and inferred from mean decay model) vs. height in plot 10.

5. Conclusion

Foliage density is a useful characteristic for describing forests. It can be used for measuring growth and yield, carbon sequestration, health, biodiversity and fire risk. Directly measuring foliage density by destructively sampling trees is expensive and unrepresentative over large areas. Photographic methods – such as aerial and hemispherical photography – provide reasonable estimates of Leaf Area Index (LAI), but are generally unable to resolve these data into a vertical distribution.

Aerial LiDAR gives a full 3D representation of the canopy and can provide this information for large areas in a short time. Waveform and discrete LiDAR over a New Zealand radiata pine forest was obtained and compared with Leaf Area Density (LAD) measurements made in 2m height intervals across ten 0.16ha sample plots. Returns in foliage were generally characterised by a skewed shape, and the hypothesis that this skew was related to foliage density was tested.

By deconvolving the waveform with the outgoing pulse shape, an expression of the surface response can be found (Jutzi and Stilla 2006). A simple model of the canopy as a semi-transparent gas was assumed, which dictates that reflectance would follow an exponential decay as per the Beer-Lambert law. By fitting exponential decays to each deconvolved waveform peak, values for the decay constant λ were obtained. In this study we tested the hypothesis that λ will characterise the density of the foliage at that location.

λ is also a function of surface slope and roughness, as is the case for intensity. λ is preferential to intensity for surface identification since it is not affected by beam attenuation higher in the canopy. Although λ cannot be used to identify each individual return, the mean value for λ shows a strong relationship to surface type when averaged over a volume. Highest values were obtained for areas of predominately ground, medium values for understory and lower values for canopy. Within the

canopy, λ can be used to estimate LAD with an R^2 of 56%. The proportion of LiDAR returns to fall in each height band can describe LAD with an R^2 of 50%, and a model utilising both decay rate and proportion of returns described 69% of the variation in LAD. This model can be used for remotely sensing foliage density in *Pinus radiata* forests above the understorey, but could be calibrated for other species and potentially even mixed species forests.

Acknowledgements

The work in this paper was funded by the Scion Capability Fund and used data collected by the Ministry for the Environment. Many thanks to Nigel Searles from MfE for use of the data, and to Andrew Dunningham, Jonathan Harrington and David Pont from Scion for their help and knowledge. Particular thanks must also go to New Zealand Aerial Mapping, in particular Tim Farrier, for providing an excellent LiDAR service and for assistance with countless queries and demands.

References

Adams, T., Brack, C., Farrier, T., Pont, D., and Brownlie, R. (2011). So you want to use LiDAR? - A guide on how to use LiDAR in forestry. *New Zealand Journal of Forestry,* 55 (4): 19–23.

Beets, P., and Lane, P. (1987). Specific leaf area of Pinus radiata as influenced by stand age, leaf age, and thinning. *New Zealand Journal of Forestry Science,* 17 (2): 283-291.

Beets, P.N., Reutebuch, S., Kimberley, M.O., Oliver, G.R., Pearce, S.H., and McGaughey, R.J. (2011). Leaf area index, biomass carbon and growth rate of radiata pine genetic types and relationships with LiDAR. *Submitted to Forests*.

Blair, J.B., and Hofton, M.A. (1999). Modeling laser altimeter return waveforms over complex vegetation using high resolution elevation data. *Geophysical Research Letters,* 26 (16): 2509-2512.

Bongers, F. (2001). Methods to assess tropical rain forest canopy structure: an overview. *Plant Ecology,* 153 (1): 263-277.

Chauve, A., Vega, C., Durrieu, S., Bretar, F., Allouis, T., Deseilligny, P., and Puech, W. (2009). Processing full-waveform lidar data in an alpine coniferous forest: assessing terrain and tree height quality. *International journal of remote sensing,* 30 (19): 27.

Donoghue, D.N.M., Watt, P.J., Cox, N.J., and Wilson, J. (2007). Remote sensing of species mixtures in conifer plantations using LiDAR height and intensity data. *Remote Sensing of Environment,* 110 (4): 509-522.

Forster, W.A., and Nairn, J. (2010). *Literature Review of Methods for Describing Plant Canopies. Contract report written for FRST Contract No. LVLX0901: Protecting NZ's environment from pesticide exposure.*

Hofton, M., Blair, J., Rabine, D., Dubayah, R., and Greim, H. (Eds.). (2006). *Using Lidar-derived 3-D Vegetation Structure Maps to Assist in the Search for the Ivory-billed Woodpecker*.

Hofton, M.A., Minster, J.B., and Blair, J.B. (2000). Decomposition of laser altimeter waveforms. *Geoscience and Remote Sensing, IEEE Transactions on,* 38 (4): 1989-1996.

Hyyppä, J., Hyyppä, H., Litkey, P., Yu, X., Haggrén, H., Rönnholm, P., Pyysalo, U., Pitkänen, J., and Maltamo, M. (2004). Algorithms and methods of airborne laser-scanning for forest measurements. *International Archives of Photogrammetry, Remote Sensing and Spatial Information Sciences,* 36 (Part 8): 1682-1750.

Jutzi, B., and Stilla, U. (2006). Characteristics of the measurement unit of a full-waveform laser system. *Revue Française de Photogrammétrie et de Télédétection,* 182 (2006-2): 17–22.

Lefsky, M.A., Cohen, W., Acker, S., Parker, G.G., Spies, T., and Harding, D. (1999). Lidar remote sensing of the canopy structure and biophysical properties of Douglas-fir western hemlock forests. *Remote Sensing of Environment,* 70 (3): 339-361.

Lim, K., Treitz, P., Wulder, M., St-Onge, B., and Flood, M. (2003). LiDAR remote sensing of forest structure. *Progress in Physical Geography,* 27 (1): 88.

Lin, Y.C., and Mills, J.P. (2010). Factors influencing pulse width of small footprint, full waveform airborne laser scanning data. *Photogrammetric engineering and remote sensing,* 76 (1): 49-59.

Madgwick, H., and Service, N.Z.F. (1981). *Above-ground dry-matter content of a young close-spaced Pinus radiata stand*: New Zealand Forest Service.

McGaughey, R. (2010) FUSION. US Forest Service, Pacific Northwest Research Station, http://www.fs.fed.us/eng/rsac/fusion/.

Morsdorf, F., Kotz, B., Meier, E., Itten, K., and Allgower, B. (2006). Estimation of LAI and fractional cover from small footprint airborne laser scanning data based on gap fraction. *Remote Sensing of Environment,* 104 (1): 50-61.

Morsdorf, F., Meier, E., Kotz, B., Itten, K.I., Dobbertin, M., and Allgower, B. (2004). LIDAR-based geometric reconstruction of boreal type forest stands at single tree level for forest and wildland fire management. *Remote Sensing of Environment,* 92 (3): 353-362.

Morsdorf, F., Nichol, C., Malthus, T., and Woodhouse, I.H. (2009). Assessing forest structural and physiological information content of multi-spectral LiDAR waveforms by radiative transfer modelling. *Remote Sensing of Environment,* 113 (10): 2152-2163.

Naesset, E. (1997). Estimating timber volume of forest stands using airborne laser scanner data* 1. *Remote Sensing of Environment,* 61 (2): 246-253.

Parrish, C.E. (2007). Vertical object extraction from full-waveform lidar data using a 3d wavelet-based appraoch. PhD, Civil and Environmental Engineering, Wisconsin-Madison, Wisconsin.

Parrish, C.E., Jeong, I., Nowak, R.D., and Smith, R. (2011). Empirical Comparison of Full-Waveform Lidar Algorithms: Range Extraction and Discrimination Performance. *Photogrammetric Engineering & Remote Sensing (in press).*

Persson, Å., Söderman, U., Töpel, J., and Ahlberg, S. (2005). Visualization and analysis of full-waveform airborne laser scanner data. *International Archives of Photogrammetry, Remote Sensing and Spatial Information Sciences,* 36 (part 3): 103-108.

Reitberger, J., Krzystek, P., and Stilla, U. (2006). Analysis of full waveform lidar data for tree species classification. *International Archives of Photogrammetry, Remote Sensing and Spatial Information Sciences,* 36 (Part 3): 228-233.

Reitberger, J., Krzystek, P., and Stilla, U. (2008). Analysis of full waveform LIDAR data for the classification of deciduous and coniferous trees. *International journal of remote sensing,* 29 (5): 1407-1431.

Riaño, D., Valladares, F., Condés, S., and Chuvieco, E. (2004). Estimation of leaf area index and covered ground from airborne laser scanner (Lidar) in two contrasting forests. *Agricultural and Forest Meteorology,* 124 (3-4): 269-275.

Stephens, P.R., Watt, P. J., Loubser, D., Haywood, A., and Kimberley, M.O.,(Ed.) (Eds.). (2007). *Estimation of carbon stocks in New Zealand planted forests using airborne scanning LiDAR.* Finland.

Wagner, W., Ullrich, A., Ducic, V., Melzer, T., and Studnicka, N. (2006). Gaussian decomposition and calibration of a novel small-footprint full-waveform digitising airborne laser scanner. *ISPRS Journal of Photogrammetry and Remote Sensing,* 60 (2): 100-112.

Watson, A. (1947). Saligia. *Journal of the Warburg and Courtauld Institutes,* 10: 148-150.